Journal of Alloys and Compounds 897 (2022) 163228

Contents lists available at ScienceDirect

Journal of Alloys and Compounds

journal homepage: www.elsevier.com/locate/jalcom

Influence of substitutions and hydrogenation on the structural and magnetic properties of $(R'R'')_2Fe_{17}$ (R', R'' = Sm, Er, Ho): Compositions with promising fundamental characteristics

I.S. Tereshina[a,*], S.V. Veselova[a], V.N. Verbetsky[a], M.A. Paukov[b,c], D.I. Gorbunov[d], E.A. Tereshina-Chitrova[c,e]

[a] Lomonosov Moscow State University, Leninskie Gory, 119991 Moscow, Russia
[b] Nuclear Fuel Cycle Department, Research Centre Rez Ltd., Hlavni 130, 25068 Husinec-Rez, Czech Republic
[c] Faculty of Mathematics and Physics, Charles University in Prague, Ke Karlovu 5, 12116 Prague, Czech Republic
[d] Dresden High Magnetic Field Laboratory (HLD-EMFL), Helmholtz-Zentrum Dresden-Rossendorf, D-01328 Dresden, Germany
[e] Institute of Physics, ASCR, 18221 Prague, Czech Republic

ARTICLE INFO

Article history:
Received 14 September 2021
Received in revised form 8 December 2021
Accepted 10 December 2021
Available online 13 December 2021

Keywords:
Intermetallic compound
Hydride
Crystal structure
Magnetization
Curie temperature
Magnetic phase transition
Exchange interaction

ABSTRACT

The structural and magnetic properties of the $(R,R')_2Fe_{17}$-type (R and R' are heavy (Ho, Er) and light (Sm) rare earth metals, respectively) compounds and the $(R,R')_2Fe_{17}H_y$ hydrides are reported. The hydrides with a high hydrogen concentration ($y \geq 4$) are obtained by direct hydrogen absorption by the intermetallics. The rhombohedral Th_2Zn_{17}-type of structure is inherent in the Sm containing parent compounds and hydrides. The unit cell increase and increased Curie temperature are characteristic of the hydrides. Magnetic properties of the samples are investigated in pulsed magnetic fields up to 60 T. Strong magnetic fields induce phase transitions in the compounds with a high content of heavy rare earth elements. The parameter of the intersublattice exchange interaction is estimated.

1. Introduction

The idea of technology based on clean hydrogen energy is currently flourishing. Hydrogen packed into a solid (metals or intermetallics) as densely as possible permits long-lasting storage, safe transportation and a release in a controlled way [1,2]. Metal hydrides synthesized by direct solid-gas reaction have excellent storage capabilities and attract attention of scientists and technologists [3]. Intermetallic compounds based on the 4f- and 3d- transition metals, e.g. $LaNi_5$ [4], are well known for their ability to absorb large amounts of hydrogen and store it in a safe way. Some of the compounds R_2Fe_{17} (R is a rare earth metal) demonstrate a fairly high hydrogenation capacity in combination with interesting and important magnetic properties. As for the latter, hydrogenation is known as a powerful tool for changing significantly physical properties of materials (not only magnetic but also mechanical, electrical etc.) [5–13]. It is therefore important to study thoroughtly the properties of hydrides before a particular material is recommended for the use in hydrogen technology (including, but not limited to, the production of permanent magnets capable of working in the hydrogen-containing media).

The maximum amount of hydrogen absorbed by R_2Fe_{17} is 5 at.H/f.u. R_2Fe_{17} compounds can crystallize in two structural modifications depending on the type of the rare earth (heavy or light). For light rare earths, the Th_2Zn_{17} structure is formed, while in the case of heavy rare earths, the structure is Th_2Ni_{17}. Some of the compounds with Rs belonging to the boundary region can have a mixed structure [14]. In the latter samples the rhombohedral or hexagonal structure can be stabilized depending on the heat treatment and/or quenching conditions. The compounds that combine both heavy and light rare-earth metals have been studied rather poorly. Depending on the ratio of the rare-earth metals in the compound, structural phase transitions can be observed [15]. In both the rhombohedral and hexagonal R_2Fe_{17} compounds the occupied sites are of two types, a 2R–4Fe site of distorted octahedral coordination, and a second

* Corresponding author.
E-mail address: tereshina@physics.msu.ru (I.S. Tereshina).

https://doi.org/10.1016/j.jallcom.2021.163228
0925-8388/

2R–2Fe site of tetrahedral coordination, yielding a maximum content of five hydrogen atoms per formula unit [16].

The magnetic structures of the R_2Fe_{17} and their interstitially modified compositions with heavy and light rare earth metals are also different [17,18]. For light Rs the magnetic structure is ferromagnetic (moments of R and Fe sublattices are co-aligned), while for heavy rare earths the magnetic structure is ferrimagnetic (i.e. the moments of the sublattices are anti-aligned with respect to each other). Application of sufficiently strong magnetic fields to the ferrimagnets may break the magnetic moments arrangement and induce a ferromagnetic state in the compounds [19–22]. Such compounds with a field-induced ferromagnetism will have the highest magnetization since the magnetic moments of heavy Rs from Gd to Tm ranging between 7 and 10 μ_B are much higher than the magnetic moments of light Rs. (For comparison, the magnetic moment for the trivalent Sm^{3+} is only 0.7 μ_B). Furthermore, inspection of the field-induced magnetic phase transitions (having the form of continuous or abrupt magnetization jumps) in the R_2Fe_{17}-type compounds allows one to obtain information on the exchange interaction between the iron and rare earth sublattices [23].

Hydrogenation often boosts the volume of R_2Fe_{17} while keeping the parent crystal structure unchanged [7]. It increases distances between the magnetoactive ions and thus affects exchange interactions in the compounds. Presence of negative exchange interactions in some of the Fe-Fe pairs leads to the very low Curie temperatures (T_C) in the parent R_2Fe_{17} despite the very high content of Fe. Hydrogenation strengthens ferromagnetic (positive) exchange interactions and increases the Curie temperatures in R_2Fe_{17}. The T_C values linearly depend on the hydrogen concentration [20,24]. As regards the problem of influence of hydrogenation on the intersublattice R-Fe exchange, it requires a detailed study. Employment of high magnetic fields for ferrimagnets in this work provides a reliable and detailed knowledge on these interactions [25]. Such information can also be obtained from analyzing Curie temperatures of the hydrides or from the expensive inelastic neutron scattering experiments [17,26]. In the former case however, the T_C increase and increased mobility of hydrogen associated with it permit only a qualitative analysis.

The present work is structured as follows. In the first part we analyze the crystal structure of the $(R,R')_2Fe_{17}$-type of compounds and their hydrides with a mixture of light and heavy R's. In the second part, we perform a comparative study of the magnetic properties of the $(R,R')_2Fe_{17}$-H and R_2Fe_{17}-H compounds with ferrimagnetic ordering in high magnetic fields and at low temperatures to deduce the effect of hydrogenation on the intersublattice exchange interactions. The effect of hydrogenation on the Curie temperature is also investigated for the new compositions.

2. Experimental details

Cast alloys Ho_2Fe_{17}, Er_2Fe_{17}, $Sm_{2-x}Ho_xFe_{17}$, x = 0.4, 0.8 and $Sm_{2-x}Er_xFe_{17}$, x = 0.2, 0.8 (Ho_2Fe_{17} (10.5 at% Ho), Er_2Fe_{17} (10.5 at% Er), $Sm_{2-x}Ho_xFe_{17}$ with x = 0.4, 0.8 (2.1; 4.2 at% Ho) and $Sm_{2-x}Er_xFe_{17}$ with x = 0.2, 0.8 (1.1; 4.2 at% Er) were prepared by induction melting of high-purity starting components (Sm, Ho, Er of 99.5% purity, Fe of 99.9%) in an argon atmosphere. In order to compensate for the loss of rare earth metals due to evaporation, excess amounts of Sm (5 wt %), Ho and Er (1–1.5 wt%) were added to initially estimated amounts of materials. Then the samples were annealed in evacuated quartz ampoules at a temperature of 1000 °C for 4–8 days for homogenization.

The chemical and phase composition of the alloys was characterized using microstructural, X-ray diffraction (XRD) and X-ray fluorescence (RFLA) analyzes. The microstructure of the polished samples before and after the annealing procedure was studied using a LEO EVO 50 XVP scanning electron microscope (SEM) equipped with an attachment for X-ray energy dispersive (EMF) analysis in the secondary electron mode. In all cases, the errors in determining the concentration of elements did not exceed 0.5 at%.

An XRD study was carried out by means of a DRON-4-07 diffractometer (U = 40 kV, I = 30 mA) using a CoKα radiation. The diffraction patterns were taken at 2Θ = 20–120° with a step of 0.05° and an exposure of 5 s per point. The diffraction profiles were refined by the full-profile Rietveld method using the Rietan 2000 program [27]. The accuracy in determining the lattice parameters was ± (0.01–0.05)%, and in establishing the mass ratio of the phases ± (5–10)%. The determination of the chemical (elemental) composition of the cast samples was carried out using a wave-dispersive X-ray spectral fluorescence spectrometer Rigaku ZSX Primus II.

Synthesis of hydrides was carried out using a hydrogenation equipment designed for this purpose by direct reaction of parent samples crushed into fine powders with a high purity hydrogen (impurity content 10^{-3}–10^{-4} wt%) obtained by decomposing $LaNi_5H_y$ hydride [28]. Hydrogenation was performed in a stainless steel chamber. Prior to hydrogenation, the surface of powder samples was degassed by evacuating the system at room temperature for two hours. Then the chamber was filled with hydrogen. The reaction with hydrogen did not begin at room temperature. Hydrogen absorption was initiated by thermally activating the sample. The sample was slowly heated to 473 K in a similar fashion to the previously studied system $R_2Fe_{17}H_y$ [13]. The reaction chamber with the sample inside heated to 453–473 K was kept for 5 h under a hydrogen pressure of 3.5 MPa. Then the heating was discontinued and the reaction chamber was kept for several hours at room temperature to reach equilibrium. At higher temperatures, the most probable scenario of interaction of parent R_2Fe_{17} or $(Sm,R)_2Fe_{17}$ (R = Ho; Er) compounds with hydrogen would be disproportionation reaction to α-Fe and R_zH (z = 2; 3) in case of binary compounds and to α-Fe and $(Sm,R)_zH$ (z = 2; 3) in case of the compound modified by substitution.

The amount of absorbed hydrogen was determined based on the difference in the gas pressure before and after the reaction, and the composition of the obtained hydrides was calculated using the van der Waals equation. The relative error in determining the hydrogen concentration is ± 0.1H/$Sm_{2-x}R_xFe_{17}$ (± 0.05 mass% H_2), ± 0.1H/R_2Fe_{17} (± 0.05 mass% H_2). The hydride was formed according to the following reaction scheme: $R_2Fe_{17} + y/2{\cdot}H_2 \rightarrow R_2Fe_{17}H_y$; $Sm_{2-x}R_xFe_{17} + y/2H_2 \rightarrow Sm_{2-x}R_xFe_{17}H_y$, where R = Ho; Er.

The maximum concentration of hydrogen, 4.6 hydrogen atoms per formula unit, was obtained for $Sm_{1.2}Er_{0.8}Fe_{17}$. Table 1 shows the results of X-ray diffraction studies of the parent samples R_2Fe_{17}, $Sm_{2-x}R_xFe_{17}$ (R = Ho, Er) and their stable hydrides. The results are in good agreement with the data obtained for similar systems [13,29–32].

Table 1
The lattice parameters, the c/a ratio, unit cell volume and relative volume change ΔV/V for R_2Fe_{17}, $Sm_{2-x}R_xFe_{17}$ (R = Ho, Er) and their hydrides.

№	Sample	*a*, Å	*c*, Å	*c*/*a*	V, Å^3	ΔV/V,%
1	Sm_2Fe_{17} [13]	8.554	12.443	1.455	788.4	–
2	$Sm_2Fe_{17}H_{4.7}$ [13]	8.682	12.550	1.446	819.2	3.9
3	Ho_2Fe_{17}	8.449(8)	8.312(2)	0.984	512.7	–
4	$Ho_2Fe_{17}H_{3.2}$	8.533(4)	8.325(1)	0.976	523.9	2.2
5	$Sm_{1.6}Ho_{0.4}Fe_{17}$	8.541(9)	12.459(5)	1.458	789.6	–
6	$Sm_{1.6}Ho_{0.4}Fe_{17}H_4$	8.649(7)	12.526(2)	1.448	815.2	3.2
7	$Sm_{1.2}Ho_{0.8}Fe_{17}$	8.522(0)	12.429(6)	1.458	783	–
8	$Sm_{1.2}Ho_{0.8}Fe_{17}H_{4.4}$	8.644(3)	12.521(5)	1.449	811.5	3.6
9	Er_2Fe_{17}	8.440(5)	8.261(3)	0.978	509.5	–
10	$Er_2Fe_{17}H_3$	8.452(2)	8.279(5)	0.979	522.2	2.5
11	$Sm_{1.8}Er_{0.2}Fe_{17}$	8.555(8)	12.453(9)	1.456	788.8	
12	$Sm_{1.8}Er_{0.2}Fe_{17}H_{4.4}$	8.632(1)	12.511(7)	1.449	815.6	3.3
13	$Sm_{1.2}Er_{0.8}Fe_{17}$	8.518(2)	12.431(4)	1.459	791.3	–
14	$Sm_{1.2}Er_{0.8}Fe_{17}H_{4.6}$	8.641(7)	12.520(1)	1.449	818.6	3.5

The Curie temperatures were determined from the temperature dependence of magnetization measured in a magnetic field of $\mu_0 H$ = 0.1 T at 290–800 K as the maximum of the temperature derivative of the magnetization, |dM/dT|. High-field magnetization measurements were performed at the Dresden High Magnetic Field Laboratory in pulsed magnetic fields up to 60 T at different temperatures [33,34]. Experimental results of M(H) were normalized to the static magnetization measurements up to 14 T, which were obtained using a commercial PPMS 14 (Quantum Design, USA) installation. The value of the critical field $\mu_0 H_{cr1}$ at T = 2 or 4.2 K was determined by the peak of the field derivative of the magnetization, |dM/dH|. The error in determining the critical field using this method was ± 0.5 T. The experimental data were processed by the mean field theory [35–37].

3. Results and discussion

3.1. Structural properties of R_2Fe_{17}–H and $(R,R')_2Fe_{17}$–H

The initial microstructure analysis and XRD of cast alloys showed that all synthesized samples were non single-phase and contained in addition to the main phase of the type 2:17, Sm-rich secondary phases (1:3 and 1:2) and α-Fe which agrees with binary phase diagrams of the R-Fe systems. By using high-temperature annealing, formation of a dominating 2:17 phase is usually achieved as a result of interaction between Fe and Sm-rich phases. Typical SEM images of as cast (*a-d*) and annealed (*e-h*) $Sm_{2-x}R_xFe_{17}$ samples are shown in Fig. 1.

The XRD study showed that the Ho_2Fe_{17} and Er_2Fe_{17} samples are nearly single-phase after annealing. The main 2:17 phase crystallizes in the structural modification Th_2Ni_{17} (space group $P6_3/mmc$). According to the SEM and XRD data, the $Sm_{2-x}Ho_xFe_{17}$ and $Sm_{2-x}Er_xFe_{17}$ alloys remained two-phase after annealing. The main 2:17 phase of $Sm_{2-x}R_xFe_{17}$ (R = Ho, Er) has a rhombohedral crystal structure of the Th_2Zn_{17} structural type (space group $R3m$). The amount of impurity phase, soft magnetic phase α-Fe, varied between 2.5% and 8% for different samples.

Obviously, the presence of α-Fe is caused by an insufficient amount of samarium during samples preparation despite our attempt to compensate for the loss of Sm by using excess amount of the metal. Table 2 lists the annealing regimes, phase composition of the samples and mass content of phases in the alloys. One can see that ingots of Ho_2Fe_{17} and $Sm_{2-x}Ho_xFe_{17}$ (x = 0.4, 0.8) after high-temperature treatment are not largely depleted in Sm upon addition of 5 wt% of Sm to the weighted batch. For $Sm_{1.2}Ho_{0.8}Fe_{17}$ with the largest amount of substituted rare earth (4.2 at% Ho), we should have probably increased the amount of added Sm in order to get the single-phase sample.

The same concerns $Sm_{1.2}Er_{0.8}Fe_{17}$ (see Table 2), for which a 5% excess of Sm was insufficient as we observe a 5 wt% of α-Fe in the sample. In case of producing $Sm_{1.8}Er_{0.2}Fe_{17}$ (1.1% Er), i.e. close to the composition Sm_2Fe_{17}, evaporation of samarium occurred more intensively than even in the sample with a higher erbium content (4.2 at% Er).

Partial substitution of Sm with heavier Ho and Er in Sm_2Fe_{17} leads to a decrease of the lattice parameters *a* and *c* due to the lanthanide contraction (Table 1). In particular, in Ho and Er-containing samples of $Sm_{2-x}R_xFe_{17}$ (R = Ho, Er), *a*, *c* decrease monotonously with increasing x. Interestingly, in the Ho-containing series the *c*/*a* ratio equals 1.458, while for the Er-series, the *c*/*a* ratio increases from 1.456 to 1.459. The unit cell volume remains practically unchanged with an increase in the R content for both systems.

The interaction of $Sm_{2-x}Ho_xFe_{17}$ and $Sm_{2-x}Er_xFe_{17}$ with H_2 was studied at a hydrogen pressure of 3.5 MPa and following the same protocols for both systems. The obtained hydrides are finely dispersed powders resistant to oxidation in air at room temperature. The XRD study showed that diffraction patterns of the samples correspond to hydride phases with a high hydrogen concentration (2: 17: H) and soft magnetic α-Fe. Fig. 2 shows typical XRD patterns of $Sm_{1.2}Ho_{0.8}Fe_{17}$ (a) and its hydride $Sm_{1.2}Ho_{0.8}Fe_{17}H_{4.4}$ (b) measured at room temperature. The absence of additional phases such as $(Sm,R)H_2$, $(Sm,R)H_3$ with R = Ho and Er excludes the possibility of hydrogen-induced phase decomposition and indicates the correct temperature regime of hydrogenation and a high degree of thermal stability of the hydrides obtained. The lattice parameters of the main 2:17 phase before and after hydrogenation are given in Table 1.

Hydrogen absorption leads to a significant increase in the unit cell volume up to 3.6% without changing the structure type of $Sm_{2-x}R_xFe_{17}$. We find anisotropic expansion of the unit cell upon hydrogenation occurring predominantly in the basal plane. This is in good agreement with the data for the hydride of parent Sm_2Fe_{17}.

It is known that possible hydrogen concentration in R_2Fe_{17} with light rare earths is 5H at./f.u. This number can be reduced to 3.5 H at./f.u. in the case of heavy rare earths [7,24]. We observe a lower hydrogen absorption capacity for the Ho-substituted $(Sm,Ho)_2Fe_{17}$ and Er-substituted $(Sm,Er)_2Fe_{17}$ samples, where the maximum concentration of absorbed hydrogen was 4.4 and 4.6H atoms per formula unit ($H/Sm_{1.2}Ho_{0.8}Fe_{17}$ = 4.4 and $H/Sm_{1.2}Er_{0.8}Fe_{17}$ = 4.6), respectively.

The reason for obtaining a smaller amounts of hydrogen in the samples is probably due to the fact that the structure becomes more compact when passing from light metals to heavier ones – the volume of interstitial sites occupied by hydrogen atoms decreases accordingly. Therefore, it is harder for the interstitial atoms to enter these sites. Based on the data in Table 1, it can be concluded that the partial replacement of samarium atoms with heavy Rs, Ho and Er in combination with hydrogenation of $Sm_{2-x}R_xFe_{17}$ affects the absorption capacity of the materials as compared to parent Sm_2Fe_{17}. And although we could have expected the amount of absorbed hydrogen by the Ho-containing alloy to be greater than that of the Er-containing one, one should also take into account the amount of impurity phase in the parent sample (higher in the Ho-containing sample) affecting the hydrogen absorption saturation.

3.2. Temperature variation of magnetization of R_2Fe_{17}–H and $(R,R')_2Fe_{17}$–H systems

Temperature dependences of magnetization of $R_2Fe_{17}Hy$ and $(R,R')_2Fe_{17}Hy$ ($0 \le y \le 4.6$) are shown in Figs. 3 and 4 and values of Curie temperatures are given in Table 3. We observe an increase in T_C after hydrogenation.

For Er_2Fe_{17} and Ho_2Fe_{17}, the Curie temperatures are in good agreement with the known literature data [13]. The Tc of hydrides depends on the hydrogen content and is extremely sensitive to the determination method. It is then possible to compare the values of Curie temperatures if the samples are measured in identical experimental conditions. For instance, Curie temperatures of $Sm_{1.6}Ho_{0.4}Fe_{17}$ and $Sm_{1.6}Ho_{0.4}Fe_{17}H_4$, are T_C = 388 K and 510, respectively. The average increase in the Curie temperature is 30–35 K for each hydrogen atom absorbed by the compounds $(Sm,R)_2Fe_{17}$ (R = Ho or Er). The Curie temperatures of these compounds are determined, mainly, by the Fe–Fe exchange interactions [7,17]. The experimental results therefore indicate strengthening of the Fe-Fe exchange interactions as a result of hydrogenation [38].

3.3. High-field magnetic properties of R_2Fe_{17}–H and $(R,R')_2Fe_{17}$–H

We studied the magnetic properties of the parent compound R_2Fe_{17} and $(Sm,R)_2Fe_{17}$ and their hydrides mainly at low temperatures in high magnetic fields (see Figs. 5–10) with the aim of determining the fundamental parameters such as saturation magnetization, critical fields of the field-induced magnetic phase

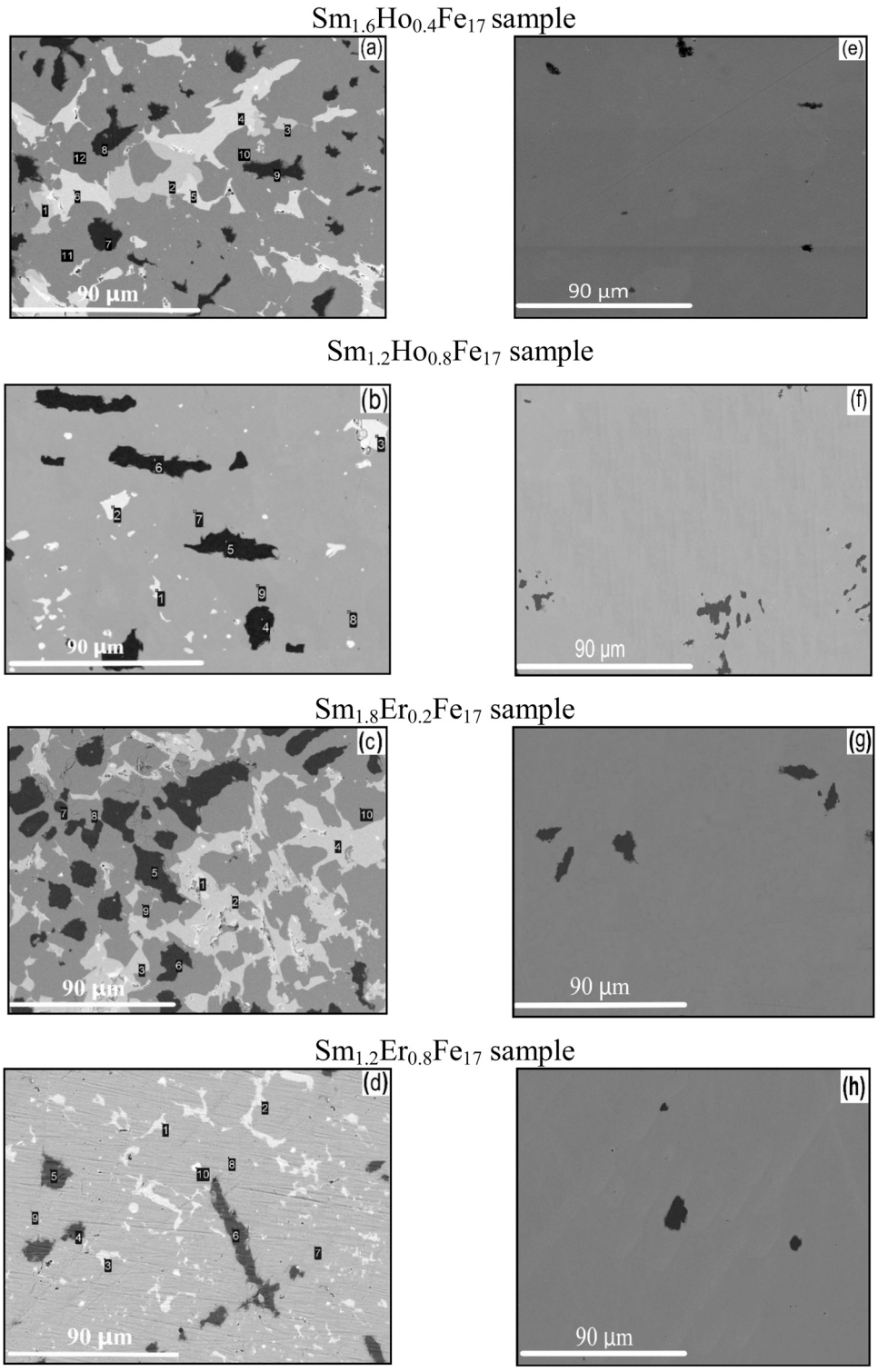

Fig. 1. SEM micrographs of $Sm_{2-x}R_xFe_{17}$ (R = Ho, Er): as-cast samples (*a-d*) and samples annealed at 1273 K (*e-h*). The phase of 2:17-type is gray, Sm-rich phase is white, α-Fe is black.

transitions and, most importantly, the inter-sublattice exchange interaction and the influence of hydrogen on it in the Th_2Ni_{17}-type (system R_2Fe_{17}-H) and Th_2Zn_{17}-type (system $(Sm,R)_2Fe_{17}$ – H) structures (see Table 3).

Fig. 5 shows the magnetization curves for Ho_2Fe_{17} and its hydride $Ho_2Fe_{17}H_{3.2}$ measured in magnetic fields up to 60 T at various temperatures. The data obtained at T = 4.2 K reveal the values of the first critical field μ_0H_{cr1} (this is the field at which the magnetization begins to increase sharply). It is seen that μ_0H_{cr1} = 42.5 and 37.5 T for the parent sample and its hydride, respectively. Thus, hydrogenation decreases μ_0H_{cr1}. The μ_0H_{cr1} values, the saturation magnetization M_S, and the parameter λ of the inter-sublattice exchange interaction, determined by the equation within the framework of the mean field theory [39,40]:

$$H_{cr1} = \lambda(M_{Fe} - 2\,M_{Ho}) \quad (1)$$

Table 2
Annealing conditions and results of phase analysis of alloys from the XRD and EDMA data.

Sample	Annealing conditions	Phase composition	Structure type	Content of phases, mass.%
Ho_2Fe_{17}	1273 K, 240 h	2:17	Th_2Ni_{17}	97
		α-Fe	*Bcc*	3
$Sm_{1.6}Ho_{0.4}Fe_{17}$	1273 K, 96 h	2:17	Th_2Zn_{17}	96
		α-Fe	*Bcc*	4
$Sm_{1.2}Ho_{0.8}Fe_{17}$	1273 K, 192 h	2:17	Th_2Zn_{17}	92
		α-Fe	*Bcc*	8
Er_2Fe_{17}	1273 K, 240 h	2:17	Th_2Ni_{17}	98
		α-Fe	*Bcc*	2
$Sm_{1.8}Er_{0.2}Fe_{17}$	1273 K, 96 h	2:17	Th_2Zn_{17}	93
		α-Fe	*Bcc*	7
$Sm_{1.2}Er_{0.8}Fe_{17}$	1273 K, 192 h	2:17	Th_2Zn_{17}	95
		α-Fe	*Bcc*	5

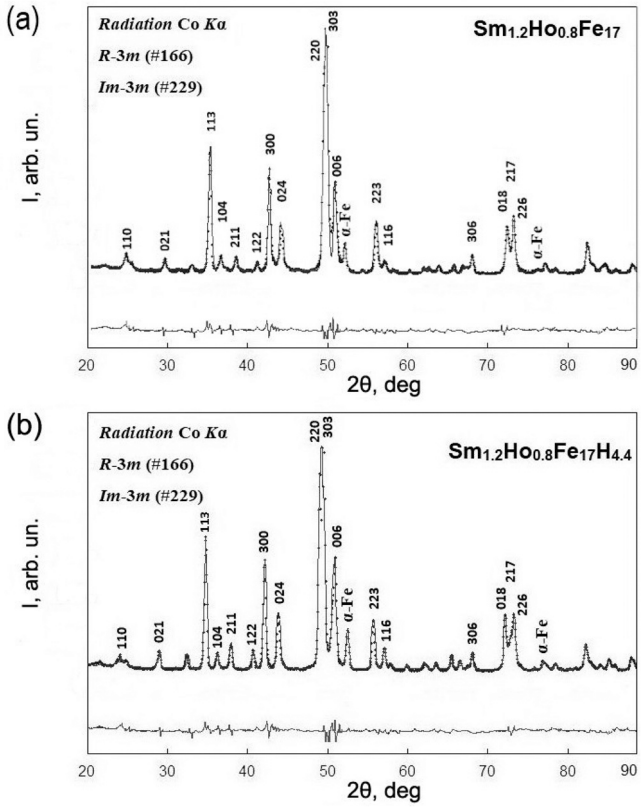

Fig. 2. Room-temperature XRD patterns of $Sm_{1.2}Ho_{0.8}Fe_{17}$ (a) and its hydride $Sm_{1.2}Ho_{0.8}Fe_{17}H_{4.4}$ (b) at room temperature: points are experimental values, the solid line is a Rietveld fit the lower curve is a difference between experiment and calculation.

where M_{Fe} and M_{Ho} are the magnetization values of the Fe and Ho sublattices, respectively (Table 3). The mean magnetic moment of Fe, μ_{Fe} = 2.0 μ_B, in the parent Ho_2Fe_{17} practically remains unchanged after hydrogenation [16,41–43]. Taking this fact into account, we can say that the parameter λ decreases from 2.6 ± 0.1 T/μ_B to 2.3 ± 0.1 T/μ_B with an increase in the hydrogen concentration in the sample from 0 to 3.2 at.H/f.u. Earlier, for the deuteride $Gd_2Fe_{17}Dy$ system, determination of exchange coupling constant J_{ex} showed that incorporation of deuterium atoms into the octahedral sites (at y ≤ 3) has practically no effect on J_{ex}, while J_{ex} drops significantly when the tetrahedral interstitial sites are filled (at y > 3).

By inspecting Fig. 5 further, one can also trace the transformation of the spin-reorientation transition induced by an external magnetic field with the increasing temperature. It can be seen that this transition (shaped as a broken M (H) curve) disappears in the parent compound Ho_2Fe_{17} much earlier than in the hydride $Ho_2Fe_{17}H_{3.2}$, being associated with an increase in the Curie temperature of the hydrogenated sample in comparison with the H-free sample.

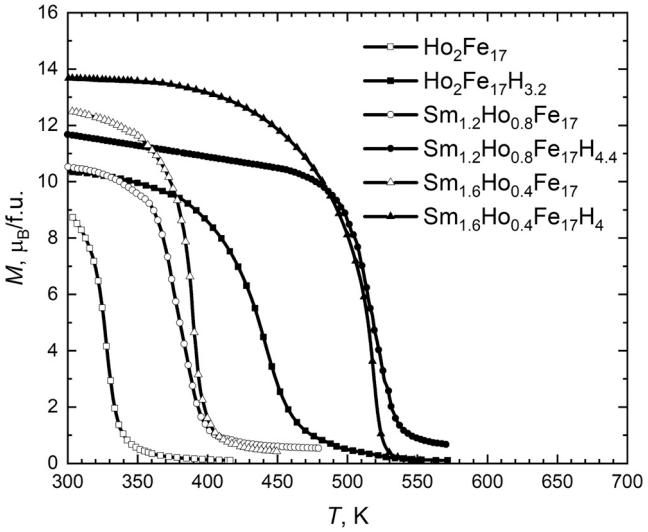

Fig. 3. Temperature dependences of magnetization of $(Sm,Ho)_2Fe_{17}$ and their hydrides in a magnetic field of μ_0H = 0.1 T.

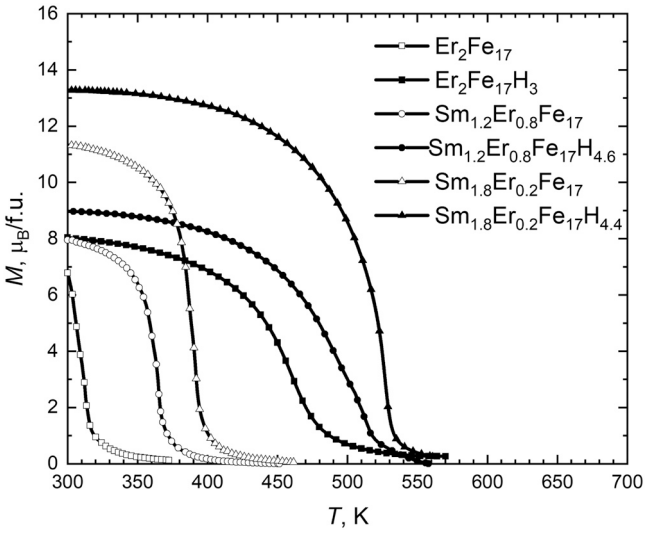

Fig. 4. Temperature dependences of magnetization of $(Sm,Er)_2Fe_{17}$ and their hydrides in a magnetic field of μ_0H = 0.1 T.

Table 3
Magnetic data of R_2Fe_{17}, $Sm_{2-x}R_xFe_{17}$ and their hydrides.

№	Composition	T_C, K	M_S, μ_B T = 2 K	μ_0H_{cr1}, T	λ, T/μ_B
1	Ho_2Fe_{17}	327	17.1	42.5	2.6
2	$Ho_2Fe_{17}H_{3.2}$	426	17.1	37.5	2.3
3	$Sm_{1.6}Ho_{0.4}Fe_{17}$	388	34.2	–	–
4	$Sm_{1.6}Ho_{0.4}Fe_{17}H_4$	510	34.1	–	–
5	$Sm_{1.2}Ho_{0.8}Fe_{17}$	383	29.9	–	–
6	$Sm_{1.2}Ho_{0.8}Fe_{17}H_{4.4}$	518	29.8	55.0	2.1
7	Er_2Fe_{17}	307	19.1	37.5	2.1
8	$Er_2Fe_{17}H_3$	404	19.1	34.0	1.9
9	$Sm_{1.8}Er_{0.2}Fe_{17}$	386	36.6	–	–
10	$Sm_{1.8}Er_{0.2}Fe_{17}H_{4.4}$	525	36.5	–	–
11	$Sm_{1.2}Er_{0.8}Fe_{17}$	362	30.7	43.5	1.6
12	$Sm_{1.2}Er_{0.8}Fe_{17}H_{4.6}$	490	30.6	41	1.5

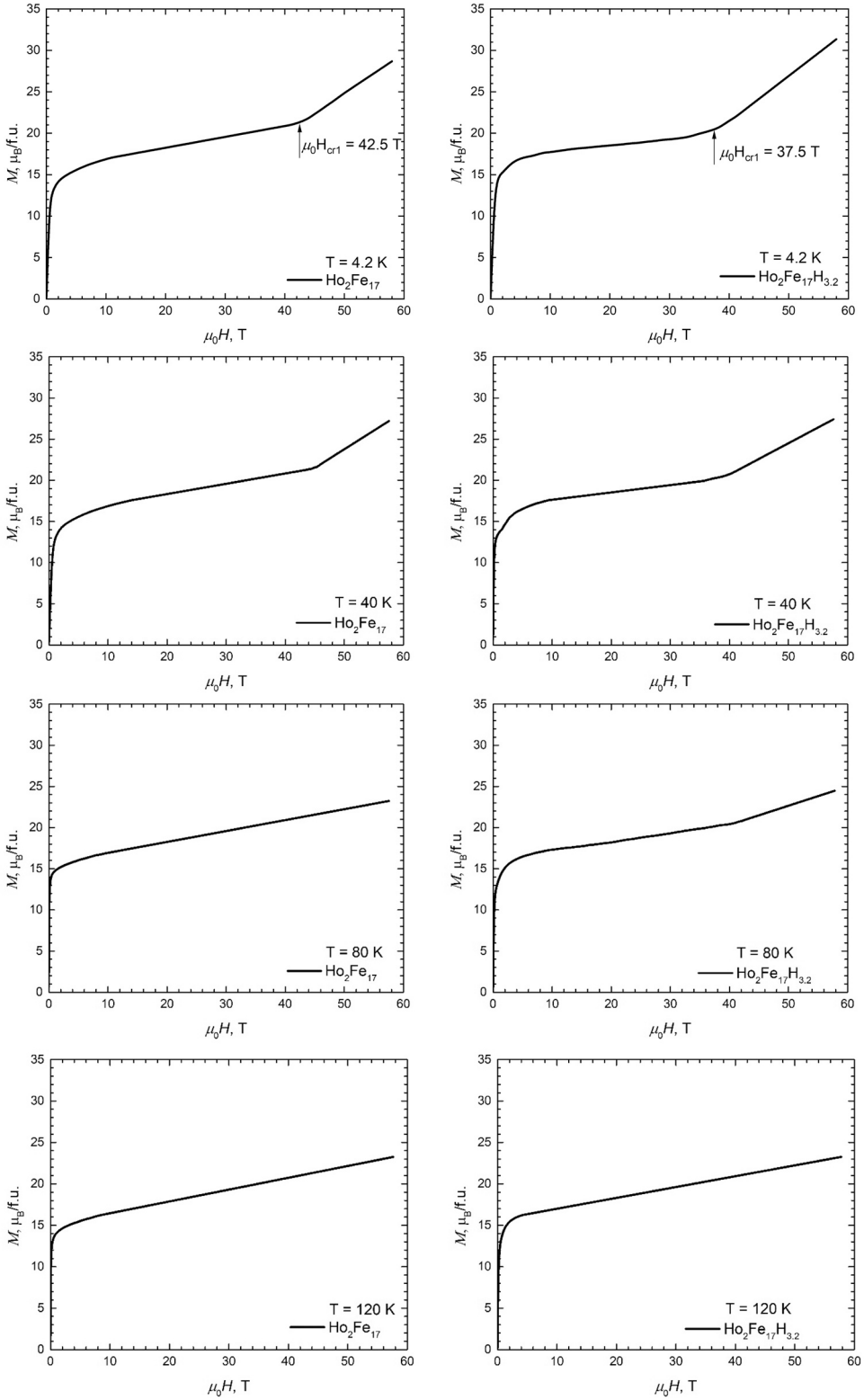

Fig. 5. Magnetization curves for Ho_2Fe_{17} and its hydride $Ho_2Fe_{17}H_{3.2}$ measured in pulsed magnetic fields at different temperatures: 4.2, 40, 80 and 120 K.

Partial substitution of Sm atoms for Ho in the $(Sm,Ho)_2Fe_{17}$ compounds leads to a significant increase in the saturation magnetization (29.9 and 34.2 μ_B, in $Sm_{1.2}Ho_{0.8}Fe_{17}$ and $Sm_{1.6}Ho_{0.4}Fe_{17}$, respectively, compared to 17.1 μ_B in Ho_2Fe_{17}) since the magnetic moments of Sm are ordered parallel to the magnetic moments of Fe atoms.

In contrast to the M(H) curves of Ho_2Fe_{17}, the M(H) curves of $Sm_{1.2}Ho_{0.8}Fe_{17}$ and $Sm_{1.6}Ho_{0.4}Fe_{17}$ demonstrate behavior characteristic of ferromagnets in fields up to 60 T (see Figs. 6 and 7). And only in the sample with a high Ho content we observe a spin-reorientation transition induced by the magnetic field as a result of hydrogenation and weakening of the intersublattice exchange. The

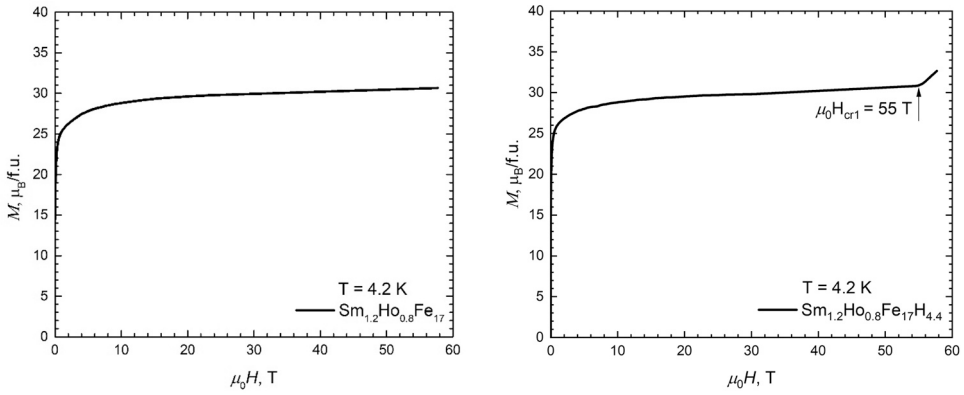

Fig. 6. Magnetization curves for $Sm_{1.2}Ho_{0.8}Fe_{17}$ and $Sm_{1.2}Ho_{0.8}Fe_{17}H_{4.4}$ measured in pulsed magnetic fields at T = 4.2 K.

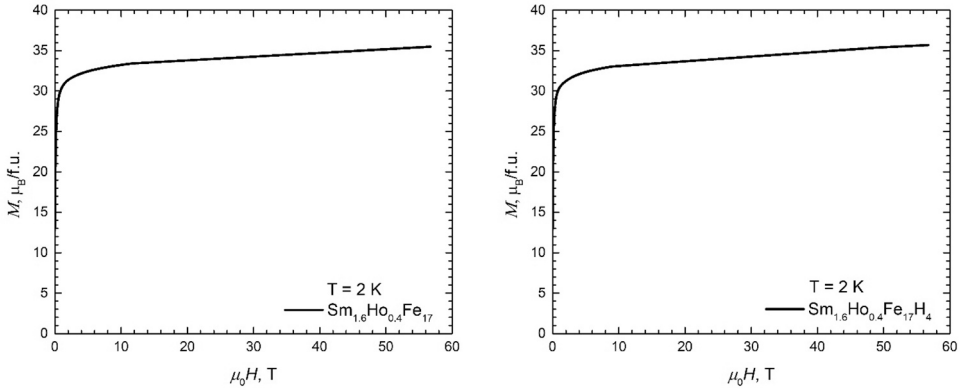

Fig. 7. Magnetization curves for $Sm_{1.6}Ho_{0.4}Fe_{17}$ и $Sm_{1.6}Ho_{0.4}Fe_{17}H_4$ measured in pulsed magnetic fields at T = 2 K.

transition field μ_0H_{cr1} is 55 T for the hydride $Sm_{1.2}Ho_{0.8}Fe_{17}H_{4.4}$. To evaluate the parameter λ of the inter-sublattice exchange interaction in this case we used a modified expression:

$$H_{cr1} = \lambda(M_{Fe} - \xi M_{Ho}) \quad (2)$$

where $\xi = x/(1 + \lambda_{Sm}\cdot\chi_{Sm})$, x is the concentration of Ho. λ_{Sm} and χ_{Sm} are the exchange parameter and susceptibility of the Sm sublattice, respectively [44]. According to our estimates, the product $\lambda_{Sm}\cdot\chi_{Sm}$ does not exceed 0.1. The magnitude of λ is 2.1 ± 0.1 T/μ_B.

By analogy with the $(Sm,Ho)_2Fe_{17}$-H system, we studied the high-field properties of the $(Sm,Er)_2Fe_{17}$-H system, including the parent compound Er_2Fe_{17} and its hydride $Er_2Fe_{17}H_3$. Fig. 8 shows the magnetization curves for Er_2Fe_{17} and $Er_2Fe_{17}H_3$ measured in magnetic fields up to 60 T at T = 4.2 K. We denote values of the first critical field μ_0H_{cr1} in the figures. It is seen that μ_0H_{cr1} = 37.5 and 34 T for the parent sample and its hydride, respectively. Thus, hydrogenation, as in the case of the Ho_2Fe_{17}-H system, leads to a decrease in the μ_0H_{cr1} value. The values of the parameter λ calculated using formula (1) are 2.1 ± 0.1 and 1.9 ± 0.1 T/μ_B for Er_2Fe_{17} and $Er_2Fe_{17}H_3$, respectively.

Partial replacement of heavy Er atoms by light Sm atoms in $(Sm,Er)_2Fe_{17}$ compounds leads to a significant increase in the saturation magnetization (30.7 and 36.6 μ_B, for $Sm_{1.2}Er_{0.8}Fe_{17}$ and $Sm_{1.8}Er_{0.2}Fe_{17}$, respectively, compared to 19.1 μ_B for Er_2Fe_{17}). Note

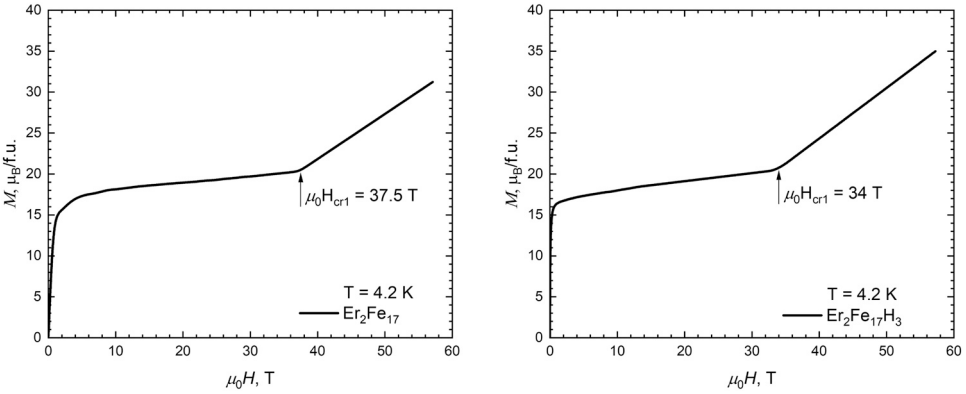

Fig. 8. Magnetization curves for Er_2Fe_{17} and $Er_2Fe_{17}H_3$ measured in pulsed magnetic fields at T = 4.2 K.

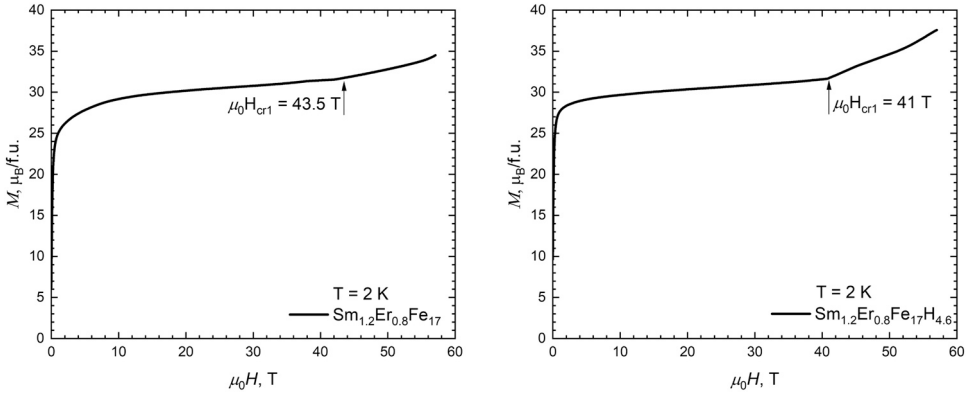

Fig. 9. Magnetization curves for $Sm_{1.2}Er_{0.8}Fe_{17}$ and $Sm_{1.2}Er_{0.8}Fe_{17}H_{4.6}$ measured in pulsed magnetic fields at T = 2 K.

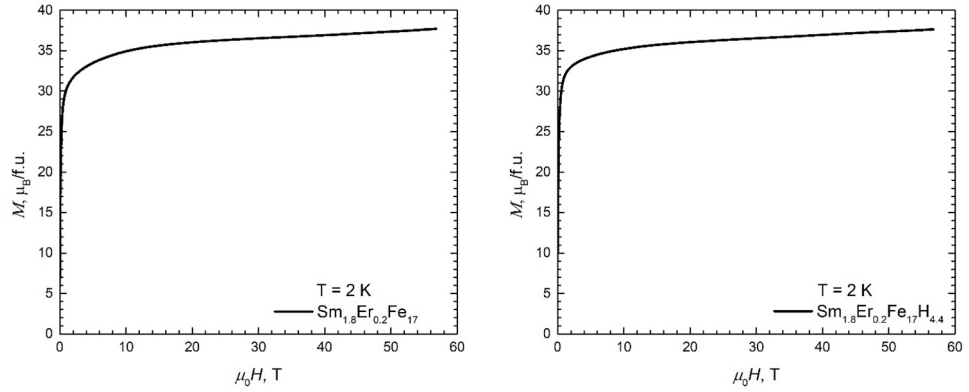

Fig. 10. Magnetization curves for $Sm_{1.8}Er_{0.2}Fe_{17}$ and $Sm_{1.8}Er_{0.2}Fe_{17}H_{4.4}$ measured in pulsed magnetic fields at T = 2 K.

that the magnetization of the corresponding hydrides practically does not change, due to the fact that Fe sublattice retains its magnetization after hydrogenation [45–47].

Fig. 9 shows M(H) curves (with denoted values of the first critical field μ_0H_{cr1}) for the substituted compositions $Sm_{1.2}Er_{0.8}Fe_{17}$ and $Sm_{1.2}Er_{0.8}Fe_{17}H_{4.6}$ at T = 4.2 K. It can be seen that μ_0H_{cr1} = 43.5 and 41 T for the parent sample and its hydride, respectively. These values are higher than those of Ho_2Fe_{17} and its hydride. We also observe a tendency towards an increase of μ_0H_{cr1} for similar compositions with holmium, namely $Sm_{1.2}Ho_{0.8}Fe_{17}$ and $Sm_{1.2}Ho_{0.8}Fe_{17}H_{4.4}$; however, in the latter case, the increase is much larger. The values of λ calculated using formula (2) are 1.6 ± 0.1 and 1.5 ± 0.1 T/μ_B for $Sm_{1.2}Er_{0.8}Fe_{17}$ and $Sm_{1.2}Er_{0.8}Fe_{17}H_{4.6}$, respectively.

We further noted that when the amount of Er substituted for Sm is sufficiently low, e.g. in $Sm_{1.8}Er_{0.2}Fe_{17}$, it is not possible to observe the spin reorientation induced by strong magnetic fields not only in the parent sample but also in the hydride $Sm_{1.8}Er_{0.2}Fe_{17}H_{4.4}$ with a high hydrogen concentration (see Fig. 10).

To summarize, when studying the high-field properties of new $(Sm,R)_2Fe_{17}$-H systems we have been able to detect a small decrease in the intersublattice R-Fe exchange interaction as a result of hydrogenation (in comparison, for example, with $(Nd,R)_2Fe_{14}B$-H systems with high hydrogen concentration [23,39,48]). Note that our research was carried out on free powder samples. High-field studies of $(Sm,R)_2Fe_{17}$-H on single-crystal samples could provide much more information, including the crystal field parameters [49,50]. Accounting for the magnetocrystalline anisotropy and use of megagauss magnetic fields are also important for the compounds under study [48].

4. Conclusions

In this work, we performed a comprehensive comparative study of the structural and magnetic properties of the four systems, R_2Fe_{17}–H and $(Sm,R)_2Fe_{17}$-H with R = Ho and Er. While $R_2Fe_{17}H_y$ ($3 \le y \le 3.2$) (stable hydrides over time [51]) have the Th_2Ni_{17}-type structure, the substituted systems with samarium $(Sm,R)_2Fe_{17}Hy$ ($4 \le y \le 4.6$) have the Th_2Zn_{17} structure. The increase in the unit cell volume as a result of hydrogenation exceeds 2% and 3%, respectively.

The average increase of the Curie temperature is ~ 30–35 K for each hydrogen atom introduced into the crystal lattice of the compounds under study. In Ho_2Fe_{17}-H, Er_2Fe_{17}-H and some compounds of the $(Sm,R)_2Fe_{17}$–H series we observed field-induced spin-reorientation phase transitions and determined the values of the first critical fields along with parameters of the intersublattice exchange interaction (within the framework of the mean field theory). Hydrogenation is found to decrease the critical field μ_0H_{cr1}, while the substitution of Sm for Ho and Er atoms on the contrary increases it.

The intersublattice exchange interaction and the measure of it, λ, decreases after hydrogenation. The substitution of Sm for heavy Rs, leads to a significant increase in the saturation magnetization of the compounds. The proposed new magnetic materials possessing sufficiently high hydrogen capacity, can be used in various fields of science and technology, e.g. as hydrogen-containing permanent magnets or as hydrogen accumulators for hydrogen technology.

Declaration of Competing Interest

The authors declare that they have no known competing financial interests or personal relationships that could have appeared to influence the work reported in this paper.

Acknowledgements

This work was partially performed within the framework of the state assignment of the Faculty of Chemistry, Moscow State University. M.V. Lomonosov Moscow State University, Russia (Agreement No. AAAA-A16-116053110012-5). Magnetic studies in steady fields were performed under the support of Project no. 19-00925S of the Czech Science Foundation, Czech Republic and by MGML (https://mgml.eu) within the Program of Czech Research Infrastructures, Czech Republic (Project no. LM2018096). For the high-field studies we acknowledge the support of HLD at HZDR, member of the European Magnetic Field Laboratory (EMFL).

References

[1] M.V. Lototskyy, I. Tolj, L. Pickering, C. Sita, F. Barbir, V. Yartys, The use of metal hydrides in fuel cell applications, Prog. Nat. Sci. Mater. Int. 27 (2017) 3–20, https://doi.org/10.1016/j.pnsc.2017.01.008

[2] V.N. Verbetsky, S.V. Mitrohin, Properties of metal-hydrides and prospects for their use, Materialovedenie 1 (2009) 48–60.

[3] P. Modi, K.-F. Aguey-Zinsou, Room temperature metal hydrides for stationary and heat storage applications: a review, Front. Energy Res. 9 (2021) 1–25, https://doi.org/10.3389/fenrg.2021.616115

[4] J.-M. Joubert, V. Paul-Boncour, F. Cuevas, J. Zhang, M. Latroche, $LaNi_5$ related AB_5 compounds: structure, properties and applications, J. Alloy. Compd. 862 (2021) 158163, https://doi.org/10.1016/j.jallcom.2020.158163

[5] G. Sandrock, R.C. Bowman, Gas-based hydride applications: recent progress and future needs, J. Alloy. Compd. 356–357 (2003) 794–799, https://doi.org/10.1016/S0925-8388(03)00090-2

[6] K.H.J. Buschow, P. Chatel, Hydrogen absorption and magnetic properties of intermetallic compounds based on 3d elements, Pure Appl. Chem. 52 (1979) 135–146.

[7] G. Wiesinger, G. Hilscher, Magnetism of hydrides, in: K.H.J. Buschow (Ed.), Handbook of Magnetic Materials, vol. 17, Elsevier, 2007, p. 293, https://doi.org/10.1016/S1567-2719(07)17005-0

[8] O. Isnard, V. Pop, Effect of hydrogen as interstitial element on the magnetic properties of some iron rich intermetallic compounds, J. Alloy. Compd. 509S (2011) S549–S554, https://doi.org/10.1016/j.jallcom.2011.01.011

[9] E.A. Tereshina, H. Drulis, Y. Skourski, I.S. Tereshina, Strong room-temperature easy-axis anisotropy in $Tb_2Fe_{17}H_3$: an exception among R_2Fe_{17} hydrides, Phys. Rev. B 87 (2013) 214425, https://doi.org/10.1103/PhysRevB.87.214425

[10] S. Nikitin, I. Tereshina, E. Tereshina, W. Suski, H. Drulis, The effect of hydrogen on the magnetocrystalline anisotropy of R_2Fe_{17} and $R(Fe,Ti)_{12}$ (R = Dy, Lu) compounds, J. Alloy. Comp. 451 (2008) 477–480, https://doi.org/10.1016/j.jallcom.2007.04.106

[11] O. Isnard, S. Miraglia, M. Guillot, D. Fruchart, High field magnetization measurements of Sm_2Fe_{17}, $Sm_2Fe_{17}N_3$, $Sm_2Fe_{17}D_5$ and Pr_2Fe_{17}, $Pr_2Fe_{17}N_3$, J. Appl. Phys. 75 (10) (1994) 5988–5993, https://doi.org/10.1063/1.355485

[12] T.S. Zhao, T.W. Lee, K.S. Pang, J.I. Lee, High-field magnetization processes in Tb_2Fe_{17} and Er_2Fe_{17}, J. Magn. Magn. Mater. 140 (144) (1995) 1009–1010.

[13] O. Isnard, S. Miraglia, J.L. Soubeyroux, D. Fruchart, P. l'Héritier, A structural analysis and some magnetic properties of the $R_2Fe_{17}H_x$ series, J. Magn. Magn. Mater. 137 (1994) 151–156, https://doi.org/10.1016/0304-8853(94)90201-1

[14] M.D. Kuz'min, Y. Skourski, K.P. Skokov, K.-H. Müller, O. Gutfleisch, Determining anisotropy constants from a first-order magnetization process in Tb2Fe17, Phys. Rev. B 77 (4) (2008) 132411, https://doi.org/10.1103/PhysRevB.77.132411

[15] A.S. Ilyushin, Introduction to the Structural Physics of Rare-Earth Intermetallic Compounds, Moscow State University, Moscow, 2005 (in Russian).

[16] O. Isnard, S. Miraglia, J.L. Soubeyroux, D. Fruchart, A. Stergiou, Neutron diffraction study of the structural and magnetic properties of the R2Fe17Hx (Dx) ternary compounds (R= Ce, Nd and Ho), J. Less Common Met. 162 (1990) 273–284.

[17] H. Fujii, H. Sun, Interstitially modified intermetallics of rare earth and 3d elements, in: K.H.J. Buschow (Ed.), Handbook of Magnetic Materials, vol. 9, Elsevier, 1995, p. 303.

[18] T. Pandey, M.-H. Du, D.S. Parker, Tuning the magnetic properties and structural stabilities of the 2-17-3 magnets $Sm_2Fe_{17}X_3$ (X=C, N) by substituting La or Ce for Sm, Phys. Rev. Appl. 9 (2018) 034002, https://doi.org/10.1103/PhysRevApplied.9.034002

[19] I.S. Tereshina, M. Doerr, Y. Skourski, E.A. Tereshina, K. Watanabe, I.V. Telegina, H. Drulis, High-field magnetization study of $R_2Fe_{17}H_3$ (R = Tb, Dy, Ho and Er) single-crystalline hydrides, IEEE Trans. Magn. 47 (10) (2011) 3617–3620, https://doi.org/10.1109/TMAG.2011.2149500

[20] E.A. Tereshina, M.D. Kuzmin, Y. Skourski, M. Doerr, W. Iwasieczko, J. Wosnitza, I.S. Tereshina, Forced-ferromagnetic state in a $Tm_2Fe_{17}H_5$ single crystal, J. Phys. Condens. Matter 29 (2017) 24LT01, https://doi.org/10.1088/1361-648X/aa70a6

[21] O. Isnard, A.V. Andreev, M.D. Kuz'min, Y. Skourski, D.I. Gorbunov, J. Wosnitza, N.V. Kudrevatykh, A. Iwasa, A. Kondo, A. Matsuo, K. Kindo, High magnetic field study of the Tm_2Fe_{17} and $Tm_2Fe_{17}D_{3.2}$ compounds, Phys. Rev. B 88 (2013) 174406, https://doi.org/10.1103/PhysRevB.88.174406

[22] O. Isnard, A.V. Andreev, O. Heczko, Y. Skourski, High magnetic field study of the $Dy_2Fe_{17}H_x$ compounds with x = 0–3.8, J. Alloy. Compd. 627 (2015) 101–107, https://doi.org/10.1016/j.jallcom.2014.12.030

[23] I.S. Tereshina, L.A. Ivanov, E.A. Tereshina-Chitrova, D.I. Gorbunov, M.A. Paukov, L. Havela, H. Drulis, S.A. Granovsky, M. Doerr, V.S. Gaviko, A.V. Andreev, Tailoring the ferrimagnetic-to-ferromagnetic transition field by interstitial and substitutional atoms in the R-Fe compounds, Intermetallics 112 (2019) 106546, https://doi.org/10.1016/j.intermet.2019.106546

[24] O. Isnard, S. Miraglia, D. Fruchart, Interstitial insertion in R_2Fe_{17}, volume effects and their correlation with the magnetic properties, J. Magn. Magn. Mater. 140–144 (1995) 981.

[25] E.A. Tereshina, I.S. Tereshina, M.D. Kuz'min, Y. Skourski, M. Doerr, O.D. Chistyakov, I.V. Telegina, H. Drulis, Variation of the intersublattice exchange coupling due to hydrogen absorption in $Er_2Fe_{14}B$: a high-field magnetization study, J. Appl. Phys. 111 (2012) 093923, https://doi.org/10.1063/1.4716007

[26] O. Isnard, A. Sippel, M. Loewenhaupt, R. Bewley, A high energy inelastic neutron scattering investigation of the Gd–Fe exchange coupling in $Gd_2Fe_{17}D_x$ (x = 0, 3 and 5), J. Phys.: Condens. Matter 13 (2001) 3533–3543.

[27] Y.I. Kim, F. Izumi, Structure refinements with a new version of the Rietveld-Refinement Program RIETAN, J. Ceram. Soc. Jpn. 102 (1994) 401–404, https://doi.org/10.2109/jcersj.102.401

[28] K.N. Semenenko, V.N. Verbetsky, S.V. Mitrokhin, V.V. Burnasheva, Investigation of hydrogen interaction with IMC of zirconium crystallizing in the structural types of Laves phases, Russ. J. Inorg. Chem. 7 (1980) 1731–1736.

[29] I.S. Tereshina, S.A. Nikitin, V.N. Verbetsky, A.A. Salamova, Transformations of magnetic phase diagram as a result of insertion of hydrogen and nitrogen atoms in the crystalline lattice of R_2Fe_{17} compounds, J. Alloy. Compd. 336 (1–2) (2002) 36–40, https://doi.org/10.1016/S0925-8388(01)01871-0

[30] S. Nikitin, W. Suski, I. Tereshina, J. Stepien-Damm, W. Iwasieczko, H. Drulis, K. Skokov, Structural and magnetic properties of $Dy_2Fe_{17}H_x$ (x = 0 and 3) single crystals, J. Alloy. Compd. 404–406 (2005) 172–175, https://doi.org/10.1016/j.jallcom.2005.03.101

[31] S.V. Veselova, I.S. Tereshina, V.N. Verbetsky, D.S. Neznakhin, E.A. Tereshina-Chitrova, T.P. Kaminskaya, A. Yu Karpenkov, O.V. Akimova, D.I. Gorbunov, A.G. Savchenko, Structure and magnetic properties of $(Sm,Ho)_2Fe_{17}N_x$ (x = 0; 2.4), J. Magn. Magn. Mater. 502 (2020) 166549, https://doi.org/10.1016/j.jmmm.2020.166549

[32] O. Tegus, Y. Lu, N. Tang, J.X. Wu, M. Yu, Q.A. Li, R.W. Zhao, Y. Jian, F. Yang, Magnetic properties of $(Sm_{1-x}R_x)_2Fe_{17}N_y$ (R=Dy, Er) compounds, IEEE Trans. Magn. 28 (1992) 2581–2583, https://doi.org/10.1109/INTMAG.1992.696380

[33] S. Zherlitsyn, B. Wustmann, T. Herrmannsdörfer, J. Wosnitza, Status of the pulsed-magnet-development program at the Dresden high magnetic field laboratory, IEEE Trans. Appl. Supercond. 22 (2012) 4300603, https://doi.org/10.1109/TASC.2012.2182975

[34] Y. Skourski, M.D. Kuz'min, K.P. Skokov, A.V. Andreev, J. Wosnitza, High-field magnetization of Ho_2Fe_{17}, Phys. Rev. B 83 (2011) 214420, https://doi.org/10.1103/PhysRevB.83.214420

[35] A. Zvezdin, Field induced phase transitions in ferrimagnets, Handbook of Magnetic Materials, vol. 9, Elsevier, Netherlands, 1995, pp. 405–543, https://doi.org/10.1016/S1567-2719(05)80008-3

[36] N.H. Duc, Intersublattice exchange coupling in the lanthanide-transition metal intermetallics, in: K.A. Gschneider Jr., L. Eyring (Eds.), Handbook on the Physics and Chemistry of Rare Earths, vol. 24, Elsevier, Amsterdam, 1997, p. 163 (Ch.).

[37] J.J.M. France, R.J. Radwanski, Magnetic properties of binary rare-earth 3d-transition-metal intermetallic compounds, Handbook of Magnetic Materials, 1993, v. 7, ed. K.H.J. Buschow (Amsterdam: North-Holland). Ch. 5, p. 307.

[38] S.V. Veselova, M.A. Paukov, I.S. Tereshina, V.N. Verbetsky, K.V. Zakharov, D.I. Gorbunov, A.N. Vasil'ev, Synthesis, structure and magnetic properties of the $Sm_{1.2}Ho_{0.8}Fe_{17}H_x$ (x = 0; 4.4), J. Rare Earths 38 (2020) 1089–1094, https://doi.org/10.1016/j.jre.2020.08.010

[39] I.S. Tereshina, A.P. Pyatakov, E.A. Tereshina-Chitrova, D.I. Gorbunov, Y. Skourski, J.M. Law, M.A. Paukov, L. Havela, M. Doerr, A.K. Zvezdin, A.V. Andreev, Probing the exchange coupling in the complex modified Ho-Fe-B compounds by high-field magnetization measurements, AIP Adv. 8 (5) (2018) 125223, https://doi.org/10.1063/1.5062588

[40] J.P. Liu, F.R. de Boer, P.F. de Chatel, R. Coehoorn, K.H.J. Buschow, On the 4f-3d exchange interaction in intermetallic compounds, J. Magn. Magn. Mater. 132 (1994) 159, https://doi.org/10.1016/0304-8853(94)90310-7

[41] D. Fruchart, O. Isnard, S. Miraglia, J.-L. Soubeyroux, Magnetic properties of the $R_2Fe_{17}H_x$ series, J. Alloy. Compd. 231 (1995) 188–194.

[42] T. Beuerle, M. Fähnle, Ab initio calculation of magnetic moments and hyperfine fields in $Y_2Fe_{17}Z_3$ (Z = H, C, N), Phys. Stat. Sol. (b) 174 (1992) 257–272.

[43] I.S. Tereshina, S.A. Nikitin, J. Stepien-Damm, L.D. Gulay, N.Y. Pankratov, A.A. Salamova, V.N. Verbetsky, W. Suski, Structural and magnetic properties of $Lu_2Fe_{17}H_x$ (x = 0; 3) single crystals, J. Alloy. Compd. 329 (1–2) (2001) 31–36, https://doi.org/10.1016/S0925-8388(01)01620-6

[44] A.K. Zvezdin, Magnetic phase transitions: field-induced (Order-to-order), in: K.H.J. Buschow (Ed.), Encyclopedia of Materials: Science and Technology, Elsevier Science, 2001, pp. 4841–4847.

[45] E.A. Tereshina, A.V. Andreev, J. Kamarad, H. Drulis, Magnetism of Lu_2Fe_{17}: the effects of Ru substitution, hydrogenation and external pressure, J. Alloy. Compd. 492 (1) (2010) 1–7, https://doi.org/10.1016/j.jallcom.2009.11.102
[46] E.A. Tereshina, H. Yoshida, A.V. Andreev, I.S. Tereshina, K. Koyama, T. Kanomata, Magnetism of a $Lu_2Fe_{17}H$ single crystal under pressure, J. Phys. Soc. Jpn. 76 (Suppl. A) (2007) 82–83, https://doi.org/10.1143/JPSJS.76SA.82
[47] O. Isnard, D. Hautot, G.J. Long, F. Grandjean, A structural, magnetic, and mossbauer spectral study of Dy_2Fe_{17} and its hydrides, J. Appl. Phys. 88 (5) (2000) 2750–2759, https://doi.org/10.1063/1.1287599
[48] N.V. Kostyuchenko, I.S. Tereshina, E.A. Tereshina-Chitrova, L.A. Ivanov, M. Paukov, D.I. Gorbunov, A.V. Andreev, M. Doerr, G.A. Politova, A.K. Zvezdin, S.V. Veselova, A.P. Pyatakov, A. Miyata, O. Drachenko, O. Portugall, Drastic reduction of the R-Fe exchange in interstitially modified $(Nd,Ho)_2Fe_{14}B$ compounds probed by megagauss magnetic fields, Phys. Rev. Mater. 5 (2021) 074404, https://doi.org/10.1103/PhysRevMaterials.5.074404
[49] A.V. Andreev, M.D. Kuzmin, S. Yoshii, E.A. Tereshina, K. Kindo, M. Hagiwara, F.R. de Boer, High-field magnetization of a $Dy_2Fe_{14}Si_3$ single crystal, J. Alloy. Compd. 509 (2011) 5042–5046, https://doi.org/10.1016/j.jallcom.2011.02.012
[50] N.V. Kostyuchenko, I.S. Tereshina, D.I. Gorbunov, E.A. Tereshina-Chitrova, K. Rogacki, A.V. Andreev, M. Doerr, G.A. Politova, A.K. Zvezdin, High-field magnetization study of $(Nd,Dy)_2Fe_{14}B$: intrinsic properties and promising compositions, Intermetallics 124 (2020) 106840, https://doi.org/10.1016/j.intermet.2020.106840
[51] M.A. Paukov, L.A. Ivanov, D.I. Gorbunov, I.S. Tereshina, Magnetic and magnetothermal properties of hydrogenated materials based on rare earths and iron, IEEE Magn. Lett. 10 (2019) 2508705, https://doi.org/10.1109/LMAG.2019.2951341